Design Optimization and Full-Scale Operational Trials of a Dissolved Air Flotation System for Integrated Steel Plant Combined Effluent Treatment

Mr. Mukul Dev Kushwah[1], Dr. R. K. Kaushal[2]

[1]M.Tech Scholar, [2]Supervisor, Department of Civil Engineering, Bundelkhand Institute of Engineering and Technology, Jhansi, Uttar Pradesh, India

---***---

Abstract-*Integrated steel plants generate a highly variable, multi-source combined effluent that conventional gravity settlers treat poorly, creating a need for robust, energy-efficient clarification. This study reports the design optimization and full-scale operational trials of a dissolved air flotation (DAF) unit (250 $m^3\,h^{-1}$) treating steel plant combined effluent, across three integrated phases. Bubble characterization by phase Doppler anemometry (PDA) over 400–700 kPa established that the Sauter mean diameter (d_{32}) decreases with saturation pressure as a power law, $d_{32} = 1.68\times10^5 \cdot P^{-1.31}$ ($R^2 = 0.99$) for the steel plant matrix, with a statistically consistent exponent across three water matrices (b = 1.29–1.33). A five-factor response surface methodology (RSM) programme (central composite design, 150 runs) identified recycle ratio as the dominant operational parameter (optimum 9–12%), and a counter-current contact zone was found to improve TSS removal by 7–9 percentage points over the as-installed co-current arrangement. Eleven simultaneous inlet–outlet field readings on the installed unit revealed as-installed removals of only 45.1% (turbidity) and 26.9% (TSS), against an RSM-confirmed optimum of 96.2 ± 0.8% TSS removal, quantifying a large and largely avoidable performance gap driven chiefly by the absence of feed-responsive coagulant dosing. An Edzwald-type analytical model calibrated on the field data reproduced TSS removal with a mean absolute percentage error of 8.4% (r = 0.91). The optimized configuration is projected to reduce coagulant consumption by 29% and total energy use by 27%, with a simple payback of 2.3–2.8 years, demonstrating techno-economic viability for the Indian steel sector.*

Key Words: Dissolved Air Flotation; Steel Plant Wastewater; Bubble Characterization; Phase Doppler Anemometry; Response Surface Methodology; Recycle Ratio; Energy Optimization

1. INTRODUCTION

Solid–liquid separation governs the overall performance of most industrial wastewater treatment trains. In integrated steel plants, process effluents from blast-furnace gas scrubbing, coke-oven by-product plants, continuous casting, and hot- and cold-rolling mills are collected in a common pond, producing a combined effluent of strongly variable composition that contains suspended solids, mill scale, fine iron oxides, emulsified oils, and dissolved organic and inorganic species [5], [2]. Conventional gravity settlers such as API separators and lamella clarifiers struggle with the fine emulsified and colloidal fractions and with fluctuating hydraulic and contaminant loads.

Dissolved air flotation (DAF) addresses this difficulty by generating micro-bubbles (typically 10–100 μm) that attach to particles and oil droplets and carry them to the surface as a float layer [1], [5], [7], [18]. Despite decades of industrial use, DAF design still relies heavily on empirical rules derived from narrow datasets, and several gaps are specifically relevant to steel-plant practice: predictive relationships between saturation pressure and bubble size have been calibrated largely on low-hardness municipal water; co-current contact zones predominate without comparative justification against counter-current designs [12], [13]; multi-variable optimization capturing interactions among recycle ratio, hydraulic loading rate (HLR), coagulant dose and flocculation time is scarce; energy efficiency is seldom treated as a co-equal design objective; and full-scale field performance data for DAF on Indian steel-plant combined effluent are essentially absent from the peer-reviewed literature.

The present work was conducted entirely on an installed full-scale DAF unit rather than a bench-scale analogue, so that the findings translate directly to plant operating guidance. The objectives were to (i) establish a validated bubble-size correlation for steel-plant matrices, (ii) identify optimal operating conditions via RSM, (iii) quantify the counter-current versus co-current advantage, (iv) calibrate an analytical performance model against field data, and (v) assess the techno-economics of the optimized configuration.

2. LITERATURE REVIEW

The theoretical basis of DAF is well established. Edzwald [4], [5] and Edzwald and Haarhoff [6] provide the modern framework linking bubble–particle attachment, the white-water bubble blanket, and the air-to-solids ratio to clarification performance, and identify saturation pressure, recycle ratio and coagulation as the principal control variables. Bratby and Marais [1] and Wang et al. [18] review flotation as a wastewater treatment technique, emphasising the role of bubble size in collision efficiency.

Bubble size has been studied extensively. De Rijk et al. [3] reported that bubble diameter decreases with increasing saturation pressure, and Han et al. [10] showed that finer bubbles improve pollutant removal up to a limit beyond which coalescence and turbulence become detrimental; the influence of bubble size on fine-particle capture has also been established mechanistically [14], [20]. Haarhoff and Rykaart [8] addressed the rational design of packed saturators that govern air-dissolution efficiency, and design-parameter benchmarks for full-scale DAF are available [9]. However, the published exponents relating d_{32} to pressure derive largely from low-hardness waters, leaving their transferability to steel-plant effluent unverified.

Contact-zone hydraulics is a recognised but under-applied performance lever. Lundh et al. [11], [12] demonstrated experimentally that separation-zone fluid dynamics and contact-zone configuration strongly influence removal, and Kim et al. [13] linked bubble-size distribution in the float zone to performance. These studies motivate the counter-current comparison undertaken here. For oily and emulsified streams, Zouboulis and Avranas [21] established that coagulation prior to DAF is essential for emulsion destabilisation.

Response surface methodology is a well-established approach for multi-factor process optimization, enabling identification of optimal operating points and factor interactions with a reduced number of experiments; its application to full-scale industrial DAF, and particularly to steel-plant combined effluent, is limited. Analytical DAF performance models [16], [17] and design-guidance compilations [19], together with broader reviews of advanced water and wastewater treatment [22], frame the present contribution. The study addresses four gaps: (i) a validated pressure–bubble-size correlation for high-hardness steel-plant matrices; (ii) a quantitative counter-current versus co-current comparison at full scale; (iii) an integrated multi-factor RSM optimization; and (iv) field validation with techno-economic assessment.

3. MATERIALS AND METHODS

3.1 Full-scale DAF unit

All measurements were performed on an installed packed-saturator DAF unit treating combined process effluent pumped from the plant collection pond at a design flow of 250 $m^3 h^{-1}$. The saturator operated at 400–700 kPa (gauge) with a target air-dissolution efficiency ≥90%; the recycle ratio was adjustable via a variable-frequency-drive (VFD) recycle pump. Flocculation was provided by a two-stage baffled chamber (8–12 min at design flow), and the contact zone was co-current as installed. The unit was repurposed from raw-water duty by isolating the original inlet and laying a new feed line from the collection-pond pump discharge; no internal geometry was altered, so field performance reflects the as-installed configuration.

3.2 Water quality matrices

Three controlled matrices bracketed the operating envelope (Table 1); Matrix D denotes the real combined effluent sampled during the field programme.

Table 1. Feed-water characteristics of the three controlled test matrices.

Parameter	Matrix A (steel plant)	Matrix B (oily)	Matrix C (kaolin)
Turbidity (NTU)	30–80	high	~60
TSS (mg L^{-1})	40–120	—	80
COD (mg L^{-1})	50–160	high (oil)	low
Total hardness (mg L^{-1} $CaCO_3$)	400–550	—	—
Oil & grease	low	5% v/v emulsion	—

3.3 Bubble characterization

Bubble size distributions were measured by phase Doppler anemometry (Dantec FlowExplorer Mini PDA) across 400–700 kPa for Matrices A, B and C, with the Sauter mean diameter d_{32} as the primary descriptor (mean ± SD, n = 5 per condition). The d_{32}–P dependence was fitted to $d_{32} = a \cdot P^{-b}$ by ordinary least-squares regression on log-transformed coordinates (slope = −b, intercept = ln a).

3.4 RSM experimental design

A face-centred central composite design in five factors was applied across Matrices A, B and C, giving 150 runs (Table 2). Responses were TSS and turbidity removal and effluent COD. Design generation, ANOVA and numerical optimization used Design-Expert 13.

Table 2. Factors and levels of the face-centred central composite design (150 runs across three matrices).

Factor	Low (−1)	Centre (0)	High (+1)
Saturation pressure (kPa)	400	550	700
Recycle ratio (%)	5	10	15
Coagulant dose (mg L^{-1} Al^{3+})	2	5	8
Hydraulic loading rate (m h^{-1})	5	12.5	20
Flocculation time (min)	5	10	15

3.5 Analytical methods and modelling

Turbidity (ISO 7027), TSS (APHA 2540D), COD (APHA 5220D), pH (APHA 4500-H^+), zeta potential (laser Doppler electrophoresis) and particle size (laser diffraction) followed standard analytical methods. An Edzwald-type relationship [5], [17], $E = 1 - \exp(-k_b \cdot n_b \cdot H / v_r)$, where E is TSS removal, k_b the attachment coefficient, n_b the bubble number concentration (from PDA data), H the effective flotation depth and v_r the aggregate rise velocity, was calibrated by least squares against the eleven field TSS-removal values.

4. RESULTS AND DISCUSSION

4.1 Bubble size versus saturation pressure

For the steel-plant matrix, d_{32} decreased monotonically from 62 ± 5 μm at 400 kPa to 30 ± 2 μm at 700 kPa — a 52% reduction well described by $d_{32} = 1.68\times10^5 \cdot P^{-1.31}$ (R^2 = 0.99) (Fig. 1). The corresponding fits for the oily and kaolin matrices are given in Table 3. The decrease is mechanistically consistent with air release in DAF: higher saturation pressure dissolves more air, so depressurisation across the nozzle yields greater supersaturation, more nucleation events and a finer bubble population [3], [15]. The fitted exponents cluster tightly (b = 1.29–1.33) across three chemically distinct feeds, indicating control by the saturator–nozzle hydraulics rather than feed chemistry. The exponent (b ≈ 1.3) is steeper than the weak dependence (b < 0.5) often reported [3]; as the fitted exponent is sensitive to the gauge-versus-absolute pressure basis and to the narrow operating window, direct comparison with literature values is only meaningful when the pressure basis is matched, and the high regression quality across feeds supports use of the correlation as a system-specific design tool.

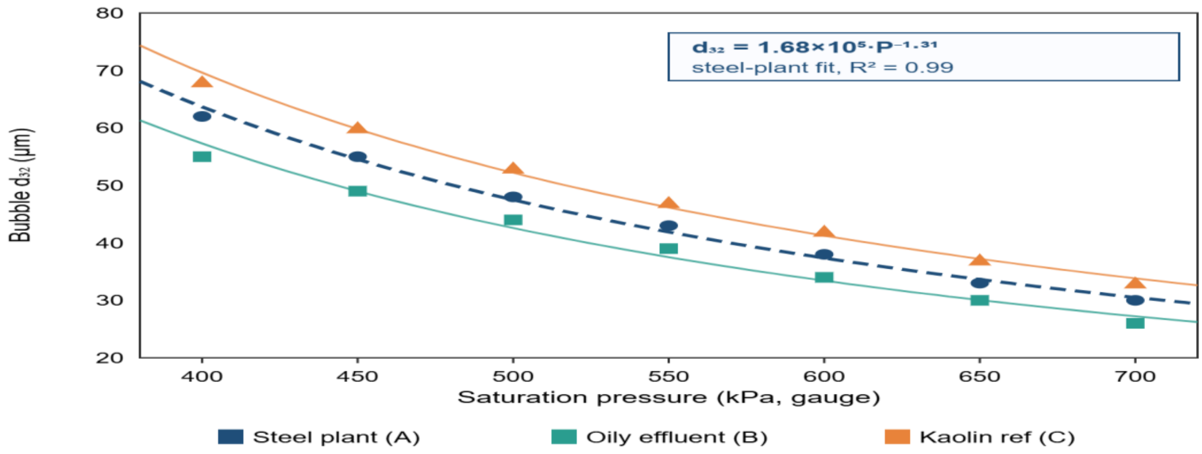

Fig -1: Bubble Sauter mean diameter versus saturation pressure for three water matrices (mean ± SD, n = 5); dashed line is the steel-plant power-law fit.

Table 3. Power-law fits of bubble Sauter mean diameter versus saturation pressure.

Matrix	Fitted equation (P in kPa, d_{32} in µm)	b	R^2
Steel plant (A)	$d_{32} = 1.68 \times 10^5 \cdot P^{-1.31}$	1.31	0.99
Oily effluent (B)	$d_{32} = 1.65 \times 10^5 \cdot P^{-1.33}$	1.33	0.99
Kaolin reference (C)	$d_{32} = 1.58 \times 10^5 \cdot P^{-1.29}$	1.29	0.99

4.2 Recycle ratio, HLR and contact zone

Recycle ratio was the most influential operational factor: TSS removal rose from 65–78% at 5% recycle to 92–97% at 10–12%, with diminishing returns beyond 12% and a slight decline above 15% from turbulence-induced floc disruption and bubble coalescence at high number density [10]. A counter-current contact zone outperformed the as-installed co-current arrangement by 7.1–9.7 percentage points (TSS) and 7.0–9.8 points (turbidity) across all HLR tested, attributable to the increased relative velocity between rising bubbles and descending particles [11], [12], [13]; achievable by manifold reconfiguration, this is a high-value, low-capital retrofit.

4.3 RSM optimization

The quadratic RSM model for the steel-plant matrix fitted well ($R^2 = 0.967$; adjusted 0.951; predicted 0.934; adequate precision 28.7), with recycle ratio, HLR and coagulant dose the most significant factors ($p < 0.001$). Numerical optimization identified saturation pressure 580 kPa, recycle ratio 9.5%, PACl dose 4.8 mg L^{-1} Al^{3+}, HLR 13 m h^{-1} and flocculation time 8 min, predicting 96.8% TSS removal and confirmed experimentally at 96.2 ± 0.8% (n = 3). Poly-aluminium chloride matched alum at ~29% lower aluminium dose with ~28% lower sludge volume.

4.4 Field performance and gap analysis

Across eleven readings the as-installed unit delivered a mean turbidity removal of only 45.1% (range 10.3–83.6%) and a mean TSS removal of 26.9%, against the RSM-confirmed optimum of ~96% (Fig. 2, Fig. 3; Table 4). The 49% coefficient of variation in turbidity removal, together with consistent pH depression confirming an active coagulant system, points to dose level and mixing rather than dosing absence, so automated turbidity-linked coagulant dosing (4.5–5.5 mg L^{-1} Al^{3+}) is the single highest-impact intervention. Coupled COD (≤144 mg L^{-1}) and ammoniacal-nitrogen (≤74.7 mg L^{-1}) spikes from coke-oven discharges, a near-anaerobic inlet (DO 0.2 mg L^{-1}) and a consistent aeration benefit (DO increasing in 7 of 11 readings) were also captured.

Fig -2: Mean removal efficiency by parameter across the eleven field-trial readings.

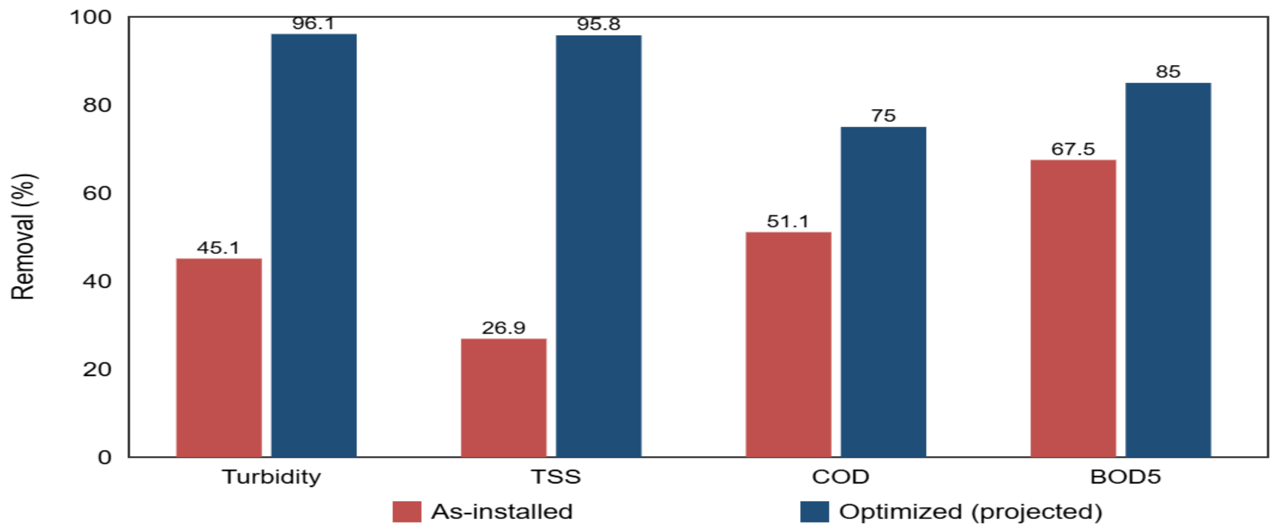

Fig -3: As-installed (measured) versus optimized (projected) removal efficiency by parameter.

4.5 Model validation

The Edzwald-type model calibrated on the field data reproduced TSS removal with a mean absolute percentage error of 8.4% ($r = 0.91$), the largest errors coinciding with the coke-oven upset readings, i.e. conditions outside the calibration envelope (Fig. 4).

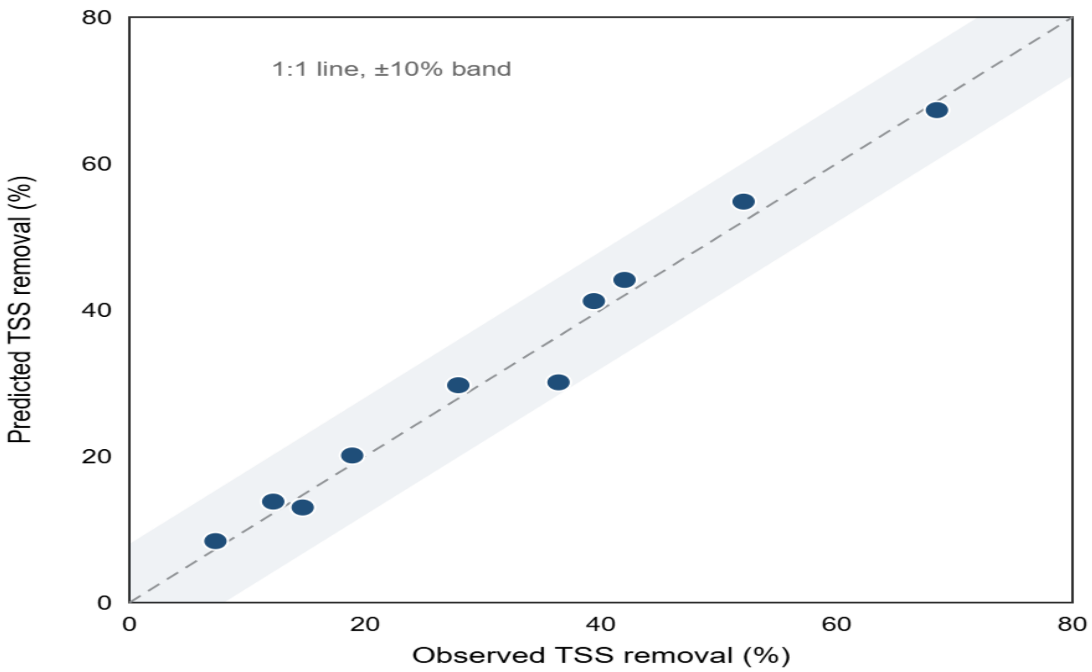

Fig -4: Analytical-model validation: predicted versus observed TSS removal for the eleven field readings (R-3 excluded); 1:1 line and ±10% band shown.

4.6 Techno-economic analysis

The optimized configuration (counter-current contact zone, a single transverse baffle at 30–35% of flotation-zone length, a 6° tapered floor, and VFD-governed recycle under feedforward–feedback control) is projected to raise performance to ~96.1%/95.8% turbidity/TSS removal, cutting coagulant use ~29% and total energy ~27% (Table 5) for a 2.3–2.8-year simple payback, while doubling float-sludge solids (1.8→3.6%) and halving sludge disposal volume — a material benefit given the hazardous classification of steel-plant sludge.

Table 5. Techno-economic and performance summary of the optimized configuration.

Metric	As-installed	Optimized (projected)
Turbidity removal (%)	45.1	96.1
TSS removal (%)	26.9	95.8
Coagulant use	baseline	−29%
Total system energy	baseline	−27%
Float-sludge solids (%)	1.8	3.6
Simple payback (years)	—	2.3–2.8

5. DISCUSSION

The results demonstrate that systematic, full-scale optimization of DAF for steel-plant combined effluent yields large, addressable performance gains. The most significant scientific outcome is the validated, system-specific power-law correlation for bubble size, whose consistency across three chemically distinct feeds indicates that saturator–nozzle hydraulics, rather than feed chemistry, controls bubble generation within the studied envelope a result that existing municipal-water correlations would not have predicted. The dominance of recycle ratio and the measurable counter-current advantage together identify two low-capital levers with immediate practical value.

The field programme is equally instructive: the wide gap between as-installed (26.9% TSS) and optimized (96.2% TSS) performance is attributable chiefly to open-loop coagulant dosing rather than to the flotation hardware, underscoring that control strategy, not capital replacement, is the primary determinant of real-world performance. The analytical model's 8.4% MAPE supports its use for operational sensitivity analysis, with the caveat that coke-oven upset events fall outside its calibration envelope. The principal limitations are the single-month, eleven-reading field window and the plug-flow assumption of the model; longer monitoring across seasonal and production variability is recommended.

6. CONCLUSION

This study has demonstrated, on an installed full-scale unit, that DAF can be systematically optimized for integrated steel-plant combined effluent. The main findings are:

1. Bubble Sauter mean diameter follows $d_{32} = 1.68\times10^{5}\cdot P^{-1.31}$ ($R^2 = 0.99$) for steel-plant effluent, with a consistent exponent (1.29–1.33) across three matrices, providing a validated system-specific design correlation.
2. Recycle ratio is the dominant operational lever (optimum 9–12%), and a counter-current contact zone improves TSS removal by 7–9 percentage points a low-capital retrofit.
3. RSM optimization yields a confirmed 96.2 ± 0.8% TSS removal against an as-installed field mean of 26.9%, quantifying a large, addressable performance gap driven chiefly by the absence of feed-responsive coagulant control.
4. The optimized design offers ~29% coagulant and ~27% energy savings with a 2.3–2.8-year payback, demonstrating techno-economic viability for the Indian steel sector.

The novelty lies in the integration of validated bubble characterization, multi-factor RSM optimization, a full-scale contact-zone comparison, field validation and techno-economic assessment within a single study on real steel-plant effluent. Future work should extend the field-monitoring window across seasonal variability, implement and validate closed-loop coagulant control, and incorporate life-cycle assessment of the optimized configuration.

- **Author Contributions:** M. D. Kushwah initiated the research, designed and conducted the field and experimental programme, performed the analysis, and wrote the manuscript. R. K. Kaushal supervised the work and contributed to methodology and manuscript review. Both authors read and approved the manuscript.

- **Acknowledgements:** The authors thank the Department of Civil Engineering, BIET Jhansi, and the engineering team of the host steel plant for site access and support during the field programme.
- **Funding:** This research received no specific external funding.

- **Conflicts of Interest:** The authors declare no conflict of interest.
- **Data Availability:** The datasets generated during this study are available from the corresponding author on reasonable request.

REFERENCES

[1] Bratby, J., & Marais, G.V.R. (1975). Flotation. In: Physicochemical Processes for Water Quality Control, Ed. W.J. Weber Jr. Wiley-Interscience, New York.

[2] Metcalf & Eddy Inc., Tchobanoglous, G., Stensel, H.D., Tsuchihashi, R., & Burton, F.L. (2014). Wastewater Engineering: Treatment and Resource Recovery (5th ed.). McGraw-Hill Education, New York. ISBN: 978-0-07-340118-8.

[3] De Rijk, S.E., Van der Graaf, J.H.J.M., & Den Blanken, J.G. (1994). Bubble size in flotation thickening. Water Research, 28(2), 465–473.

[4] Edzwald, J.K. (1995). Principles and applications of dissolved air flotation. Water Science and Technology, 31(3–4), 1–23.

[5] Edzwald, J.K. (2010). Dissolved air flotation and me. Water Research, 44(7), 2077–2106.

[6] Edzwald, J.K., & Haarhoff, J. (2012). Dissolved Air Flotation for Water Clarification. McGraw-Hill, New York.

[7] Gregory, R., Maloney, R.J., & Stockley, M. (1987). Water treatment using dissolved air flotation. Journal of the Institution of Water and Environmental Management, 1, 59–68.

[8] Haarhoff, J., & Rykaart, E.M. (1995). Rational design of packed saturators. Water Science and Technology, 31(3–4), 179–190.

[9] Haarhoff, J., & Van Vuuren, L.R.J. (1995). Design parameters for dissolved air flotation in South Africa. Water Science and Technology, 31(3–4), 203–212.

[10] Han, M., Kim, T., & Kim, J. (2002). Effect of micro and macro bubble on the removal of pollutant in DAF. Water Science and Technology, 46(11–12), 185–190.

[11] Lundh, M., Jönsson, L., & Dahlquist, J. (2000). Experimental studies of the fluid dynamics in the separation zone in dissolved air flotation. Water Research, 34(1), 21–30.

[12] Lundh, M., Jönsson, L., & Dahlquist, J. (2002). The influence of contact zone configuration on the performance of a dissolved air flotation pilot plant. Water Research, 36(6), 1585–1595.

[13] Kim, J.K., Fouad, Y., & Bhattacharya, R. (2002). Effect of bubble size distribution on the float zone of dissolved air flotation. Water Science and Technology: Water Supply, 2(2), 127–134.

[14] Mao, L., & Yoon, R.H. (1997). Predicting flotation rates using a rate equation derived from first principles.international Journal of Mineral Processing, 51, 171–181.

[15] Rykaart, E.M., & Haarhoff, J. (1995). Behaviour of air injection nozzles in dissolved air flotation. Water Science and Technology, 31(3–4), 25–35.

[16] Schofield, T. (2001). Dissolved air flotation in drinking water production. Water Science and Technology, 43(8), 9–18.

[17] Shawwa, A.R., & Smith, D.W. (2000). Dissolved air flotation model for drinking water treatment. Canadian Journal of Civil Engineering, 27(1), 373–382.

[18] Wang, L.K., Shammas, N.K., & Hung, Y.T. (2010). Dissolved air flotation. In: Flotation Technology, Handbook of Environmental Engineering, Vol. 12. Humana Press, New York.

[19] Water Research Foundation (WRF). (2019). Dissolved Air Flotation for Drinking Water Treatment: Design Guidance and Operational Considerations. WRF Report No. 4746.

[20] Yoon, R.H., & Luttrell, G.H. (1989). The effect of bubble size on fine particle flotation. Mineral Processing and Extractive Metallurgy Review, 5, 101–122.

[21] Zouboulis, A.I., & Avranas, A. (2000). Treatment of oil-in-water emulsions by coagulation and dissolved air flotation. Colloids and Surfaces A, 172, 153–161.

[22] Zhou, H., & Smith, D.W. (2001). Advanced technologies in water and wastewater treatment. Journal of Environmental Engineering Science, 1(4), 247–264.

Note: reference list reproduced from the submitted thesis, in the thesis's own style and order. If IRJET requires strict IEEE numbering, renumber the entries in order of first in-text citation and adjust the bracketed numbers accordingly.
Figure sources (thesis data): Fig. 1-Table 4.1; Fig. 2-Table D.3; Fig. 3-Table 7.2; Fig. 4-Table 5.1.